

# ABSTRACT:

## Unstructured Grid Simulations of Flow Separation Control Using Plasma Actuators

R.P. LeBeau\*, D.A. Reasor†

*Dept. of Mechanical Engineering, University of Kentucky, Lexington, KY 40506, U.S.A*

Y.B. Suzen‡

*Dept. of Mechanical Engineering & Applied Mechanics, North Dakota State University, Fargo, ND 58105, U.S.A.*

J.D. Jacob§

*Mechanical & Aerospace Engineering, Oklahoma State University, Stillwater, OK 74078, U.S.A*

P.G. Huang¶

*Dept. of Mechanical Engineering, Wright State University, Dayton, OH 45435, U.S.A*

The use of actuators has been seen as an effective means for controlling flow over plates, airfoils, and turbine blades. The use of plasma actuators is attractive since it lacks moving parts and can be easily integrated onto different geometries. There have been many experiments dealing with boundary layer control using passive elements, such as tripping the flow with surface roughness or other means of perturbing the surface without the addition of an external source of energy. There have also been many different active methods for controlling the boundary layer; examples include the use of piezoelectric actuators and morphing surfaces. Unlike many of the active methods listed above, plasma actuators are attractive because they can be easily implemented on a number of different geometries. Plasma Actuators have been proved, experimentally and numerically, as a potentially effective method for boundary layer control. This boundary layer control is driven by a body force vector tangent to the surface where the actuator is integrated. The purpose of this paper is to introduce the mathematical models used to describe the phenomena associated with plasma actuators, to implement them in a three-dimensional unstructured grid code, and to verify it by comparing numerical and experimental results.

### Nomenclature

$\vec{E}$	=	Electric Field (N/C)
$\varepsilon$	=	permittivity
$\varepsilon_r$	=	relative permittivity
$\varepsilon_o$	=	permittivity of free space, $8.854 \times 10^{-12} C^2/Nm^2$
$\vec{f}_b$	=	body force vector, $N/m^3$
FSTI	=	freestream turbulence intensity, %

---

\*Assistant Professor; Senior Member AIAA; [rplebeau@engr.uky.edu](mailto:rplebeau@engr.uky.edu).

†Graduate Student; Student Member AIAA; [dareas0@engr.uky.edu](mailto:dareas0@engr.uky.edu).

‡Assistant Professor; Senior Member AIAA; [Bora.Suzen@ndsu.edu](mailto:Bora.Suzen@ndsu.edu).

§Associate Professor; Senior Member AIAA; [jdjacob@okstate.edu](mailto:jdjacob@okstate.edu).

¶Department Chair, Senior Member AIAA; [george.huang@wright.edu](mailto:george.huang@wright.edu).

Copyright © 2007 by the authors. Published by the American Institute of Aeronautics and Astronautics, Inc. with permission.

$\Phi$	=	total scalar electric potential, Volt
$\phi$	=	electric potential due to external electric field, Volt
$\varphi$	=	electric potential due to net charge density, Volt
$k$	=	Boltzmann's constant
$L_e$	=	electrode length,m
$\lambda_d$	=	Debye length,m
$\mu$	=	location parameter for Gaussian distribution
$\mu_o$	=	permeability of free space, $4\pi \times 10^{-7}H/m$
$\omega$	=	frequency,Hz
$e$	=	elementary charge, C
$T_e$	=	near thermal equilibrium temperature for electrons in discharges, Volts
Re	=	Reynold's number based on inlet velocity and axial chord
$\rho_c$	=	net charge density, $C/m^3$
$\sigma$	=	scale parameter for Gaussian distribution
$t$	=	time, seconds
$U_{in}$	=	inlet velocity
$U$	=	streamwise velocity
$x, y, z$	=	cartesian coordinates
$y_n$	=	wall normal distance

## I. Introduction

Many different applications have been developed to assist in flow control and boundary layer control. One of the most beneficial areas for these applications is on the surface of wings and turbine blades. The integration of plasma actuators on the surface of these types of geometries can improve the efficiency and the performance of these important parts of planes and gas turbine engines respectively. Several researchers have investigated the effects of plasma actuators in these types of applications.<sup>1,2,3,4,5,6,7</sup> There have been many successful laboratory studies for these types of applications,<sup>1,8,9</sup> but few if any have been incorporated into current applications.<sup>10</sup> A schematic of the experimental setup of a plasma actuator can be seen in Figure 1. Plasma actuators essentially inject momentum tangent to the surface they are mounted on. This has been modeled as a body force vector in the vicinity above the embedded electrode. Furthermore, the effort to develop a standard for the mathematical model that describes the phenomena associated with plasma actuators has been neglected. This paper aim to describe the developement of a mathematical model for this phenomena for use in computational fluid dynamics (CFD). This paper describes the incorporation of a mathematical model into an two-dimensional and three-dimensional, incompressible, unstructured code.

There have been many two-dimensional PIV measurements done to verify the effects that plasma actuators have on the boundary layer of many different flow regimes.<sup>1</sup> In these investigations it has been shown that plasma actuators control the boundary layer by addition of momentum in the flow near the wall. As stated before, plasma actuators are active flow control devices that require external energy. They require a voltage source capable of reaching 15kV, but draw very little current resulting in a relatively low power device. The implementation of such a voltage source has made integration somewhat difficult in small scale applications such as UAVs. Nevertheless, there has been numerous findings that show that there is a lot to be gained from the integration of plasma actuators in these types of applications.

Numerical simulations of plasma actuators done on the structured grid based code GHOST, developed by Y.B. Suzen and P.G. Huang at the University of Kentucky, have been verified by experimental results.<sup>1,10,11</sup> These computations were done by calculating the body force vector as the product of the electric potential in the computational domain with that of the net charge density in the working fluid. Appropriate Neumann and Dirichlet boundary conditions were also considered at the boundaries of different parts of the domain (i.e. electrodes, solid dielectric, and fluid). The body force was then inserted as a source term in the momentum computations. This model's developement is based on Maxwell's equations and the characteristic length of plasma. The boundary condition that serves as a source in the net charge density

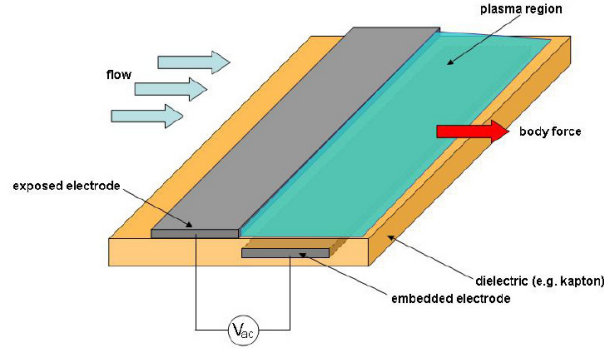


Figure 1. Schematic of plasma actuator.

computations is seen as preliminary and has not been verified for all cases. So far, this boundary condition is fixed as a half-Gaussian or full-Gaussian distribution on the surface of the dielectric directly above the embedded electrode.

## II. Modeling of Plasma Actuators

The adaption of plasma actuators into the Navier-Stokes equations was done as incorporating the product of the charge density and the electric field as a body force vector in the the location above the embedded electrode on the surface where the dielectric material meets that of the fluid. This may be expressed as

$$\vec{f}_b = \rho_c \vec{E}. \quad (1)$$

From Maxwell's Equations we know that

$$\nabla \times \vec{E} = -\mu_o \frac{\partial \vec{H}}{\partial t}, \quad (2)$$

and if we assume that the time derivative of the magnetic field,  $\vec{H}$ , is very small, a valid assumption for plasma applications, then equation (2) yields  $\nabla \times \vec{E} \sim 0$ . This implies that  $\vec{E}$  is the gradient of the scalar potential

$$\vec{E} = -\nabla \Phi. \quad (3)$$

If we assume that the permittivity  $\varepsilon$  has a non-zero spatial derivative then Gauss's law becomes

$$\nabla \cdot (\varepsilon \vec{E}) = \rho_c. \quad (4)$$

Combining equation (3) and equation (4) yields

$$\nabla \cdot (\varepsilon \nabla \Phi) = -\rho_c. \quad (5)$$

The permittivity can further be expressed as  $\varepsilon = \varepsilon_r \varepsilon_o$  where  $\varepsilon_r$  is the permittivity of the medium of interest and  $\varepsilon_o$  is the permittivity of free space. It is of interest to introduce the characteristic length of a plasma which is the Debye length,  $\lambda_d$ . The Debye length is the distance scale on which significant charge densities can spontaneously exist. We should also note that our smallest grid spacing should be no larger than this length scale in the vicinity of the plasma above the embedded electrode. The Debye length can be given by the expression

$$\lambda_d = \left( \frac{\varepsilon_o T_e}{e n_o} \right)^{1/2}. \quad (6)$$

We now introduce the following relationship for the Debye length

$$\rho_c / \varepsilon_o = (-1 / \lambda_d^2) \Phi. \quad (7)$$

Using superposition we can break the scalar potential into the potential due to the electric field and the potential due to the net charge density.

$$\Phi = \phi + \varphi. \quad (8)$$

We now have a partial differential equation for the potential due to the electric field,

$$\nabla \cdot (\varepsilon_r \nabla \phi) = 0. \quad (9)$$

The partial differential equation associated with the potential due to net charge density can be written

$$\nabla \cdot (\varepsilon_r \nabla \varphi) = -(\rho_c / \varepsilon_o). \quad (10)$$

In turn, we can write a partial differential equation for the net charge density,

$$\nabla \cdot (\varepsilon_r \nabla \rho_c) = -(\rho_c / \lambda_d). \quad (11)$$

Once we have solved the PDE describing the potential due to the change in the electric field and the PDE describing the change in the net charge density we can calculate the body force vector that will be inserted into the Navier-Stokes computation, yielding

$$\vec{f}_b = \rho_c \vec{E} = \rho_c (-\nabla \phi). \quad (12)$$

### A. Boundary Conditions

The boundary conditions given for equation 9 are to set the normal derivative to zero on the outer boundaries of the computational domain, to  $\phi(t)$  on the exposed electrode, to zero inside the embedded electrode. The value for the permittivity is taken as the harmonic mean at the boundary separating the dielectric and the air. A summary of these boundary conditions can be seen in figure 2a. A clearer representation of the permittivity at the dielectric-air boundary can be seen as:

$$\varepsilon_r = \frac{\varepsilon_{r1} \Delta V_2 + \varepsilon_{r2} \Delta V_1}{\Delta V_1 + \Delta V_2}. \quad (13)$$

One finite volume is located in the part of the domain with the defined properties for air and the other is located in the part of the domain with the defined properties for the dielectric. The boundary conditions given for equation 11 are a prescribed value of zero on the outer boundaries. The normal derivatives on the dielectric-air boundary are set to zero as well, except on the part of the boundary above the embedded electrode. It is precisely this area of interest that has the most ambiguity. A summary of the boundary conditions for equation 11 can be seen in figure 2b. The choice for the boundary conditions are consistent with the fact that we can find analytic solutions to equations 9 and 11 in rectangular domains with Dirchlet, Neumann, or Robin type boundary conditions.

## III. Results and Discussion

### A. Computations using GHOST

This modeling approach for plasma actuators is implemented in the GHOST code developed at University of Kentucky. GHOST is a pressure-based code based on SIMPLE algorithm with second order accuracy in both time and space. This code is capable of handling complex geometries, moving and overset grids, and includes multiprocessor computation capability using MPI. The overset grid capability of the code enables incorporation of plasma actuators into the computations with relative ease since electrodes can be defined as individual solid blocks. The domain can be divided into two separate computational domains: one for the air side and the other for the dielectric wall. The GHOST code has been previously validated against a wide range of test cases and flow conditions and has been used extensively in several low pressure turbine related publications.<sup>12,13</sup>

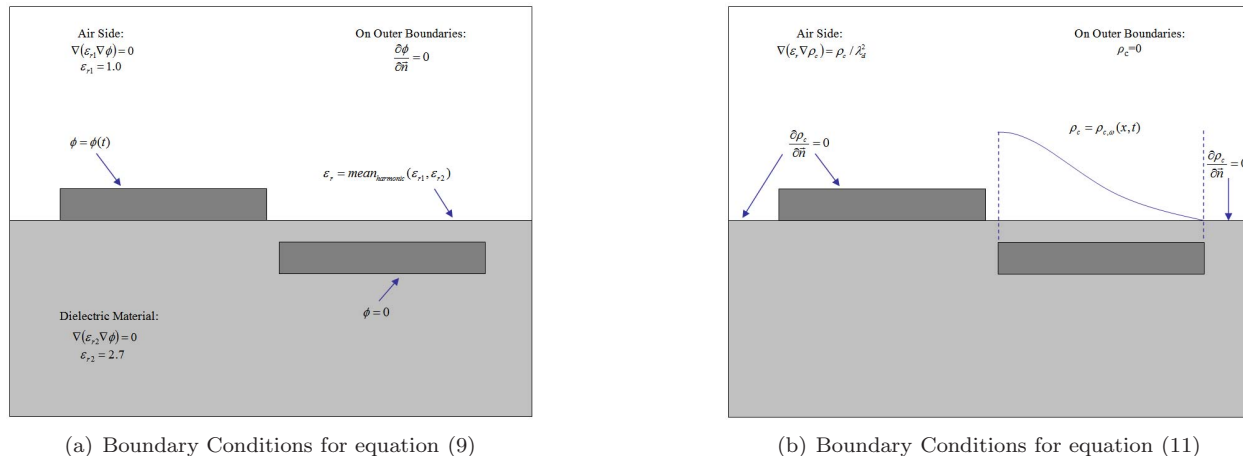


Figure 2. Boundary Conditions for Uncoupled Equations

## B. Model Calibration and Validation

In order to calibrate the parameters Debye length,  $\lambda_d$ , and the maximum charge density on the wall,  $\rho_c^{max}$ , appearing in the model we employed the quiescent flow experiments<sup>14</sup> conducted using a single pair of electrodes to better isolate the effects of the actuator on the surrounding air. The details of the actuator geometry and experimental set up are given in Reference.<sup>11</sup> The actuator consists of two 10mm wide, 0.102mm thick conductive copper strips as electrodes which are separated by a 0.127mm thick Kapton dielectric with a  $\epsilon_r$  value of 2.7. Streamwise spacing of electrodes is 0.5mm.

In the experiments the lower electrode was grounded and plasma region was generated using a square wave with frequency of,  $\omega=4.5$  kHz and amplitude of  $\phi^{max}=5$  kV. It should be noted that the experimental data is preliminary and it is used here only to demonstrate the proof of concept for the modeling approach. In the computations our aim was to match the maximum velocity observed in the experiments as well as the experimentally observed flow pattern shown in Figure (3a). From the experiment it was observed that the flow was drawn into the surface region above the embedded electrode by the plasma induced body force. This resulted in a jet issuing to the right of the actuator with a maximum velocity of approximately 1m/s.

Based on the flow pattern and maximum velocity criteria, a choice of the parameter values of  $\lambda_d=0.001$ m and  $\phi^{max}=0.0008$ C/m<sup>3</sup> seems to agree well with the experiment. The streamlines obtained from the computation using these values are shown in Figure (3b). Although not an exact match, the computed flow pattern compares favorably with the experimental flow field shown in Figure (3a). The computed maximum velocity is 1m/s also matching the experimental value. It should be noted that the boundary layer obtained by the computation appears to be thinner than the experimental data. Although the thickness could be adjusted by increasing the value of the Debye length,  $\lambda_d$  we did not attempt to do so because the experimental data may be contaminated by 3-D effects caused by the experimental setup.

The computed electric potential distribution in the vicinity of the electrodes obtained from equation 9 is shown in Figure (4) along with the streamlines of the actuator induced flow. The computed electric potentials show that the strongest electric potential variation, or the electric field, is in the region between the two electrodes. This is also the region where the strongest concentration of plasma is observed in the experiments. The streamlines indicate that the flow is pulled from above into this region and jetted to the right direction as observed experimentally.

## C. Computations using UNCLE

UNCLE is a two/three-dimensional, finite-volume, unstructured incompressible Navier-Stokes solver for steady and unsteady flow fields. UNCLE relies on a cell-centered pressure-based method that is based on the SIMPLE algorithm with second order accuracy in both time and space. In order to compute numerical flux on interfaces, a second order upwind scheme is adopted to compute advection terms and second

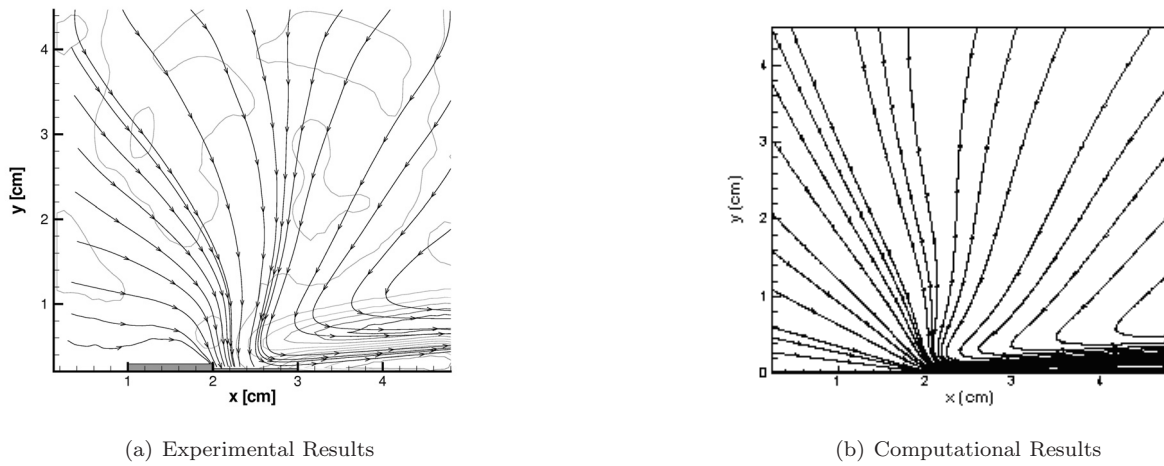


Figure 3. Comparison of experimental<sup>14</sup> and computed streamlines for the plasma actuator in quiescent flow.

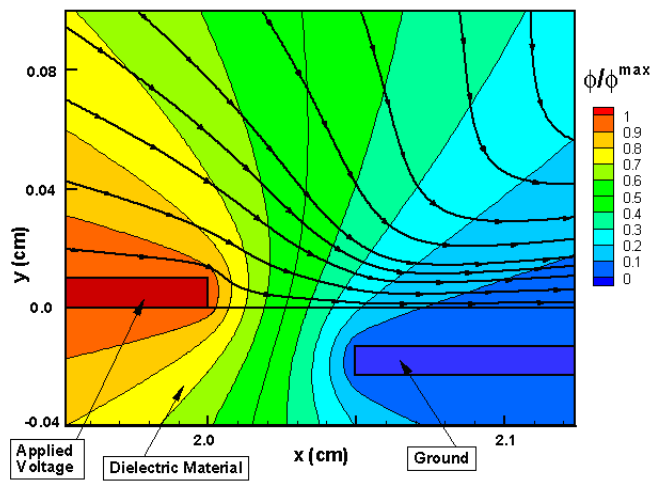


Figure 4. Computed electric potential contours and streamlines in the vicinity of the electrodes.

order central difference scheme is used for diffusion terms. A collocated grid system with the Rhie and Chow momentum interpolation method<sup>15</sup> is employed to avoid the checkerboard solution of the pressure based scheme. Fluxes on the volume faces are determined through interpolation of cell-centered values. The time discretization is a second-order fully implicit scheme. For the applications with plasma actuators, the voltage is implemented with the same numerical scheme throughout the entire numerical domain and the net charge density is implemented in areas outside of electrode or dielectric regions.

#### D. Preliminary Results using UNCLE

Thus far, results from UNCLE include the calculation of the  $\phi/\phi^{max}$  distribution through two-dimensional domains. The results obtained from simulations with GHOST are very similar to that calculated in UNCLE. In Figure 4 and 5 we can see the  $\phi/\phi^{max}$  contours which are calculated by computing the results for equation 9.

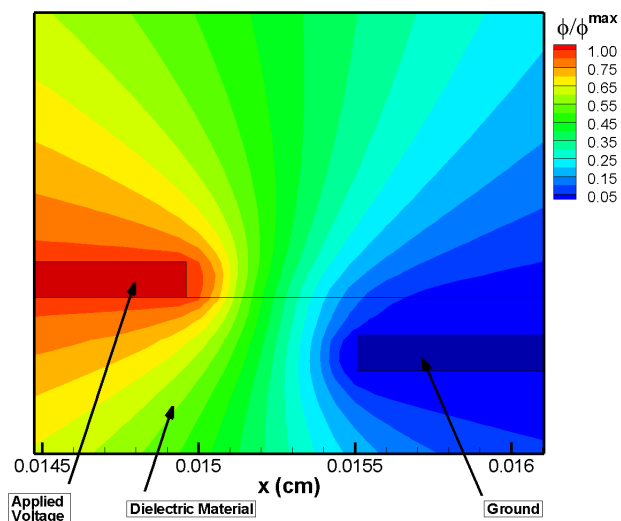


Figure 5. Computed electric potential contours and streamlines in the vicinity of the electrodes.

### IV. Concluding Remarks

The final paper will discuss detailed results from 2D and 3D simulations done on unstructured grids. The two-dimensional results obtained from the unstructured code, UNCLE, will be compared to computations done by the structured two-dimensional code, GHOST, such as those presented in ref[10]. Results will also be compared to experimental results like those of ref[1].

### Acknowledgments

This work is done with funding from NASA Glenn Research Center and the Kentucky Space Grant Consortium.

## References

- <sup>1</sup>A. Santhanakrishnan, J.D. Jacob “Flow Control Using Plasma Actuators and Linear/Annular Plasma Synthetic Jet Actuators” AIAA Paper 2006-3033, 3rd AIAA Flow Control Conference, San Francisco, CA, June 2006.
- <sup>2</sup>J.P. Boeuf, L.C. Pitchford “Electrohydrodynamic force and aerodynamic flow acceleration in surface dielectric discharge.” Journal of Applied Physics, Vol. XX, Num. XX, 2005.
- <sup>3</sup>M. Post, T. Corke, “Flow Control with Single Dielectric Barrier Plasma Actuators” AIAA Paper 2005-4630, 35th AIAA Fluid Dynamics Conference and Exhibit, Toronto, Ontario, June 6-9, 2005.
- <sup>4</sup>M. Patel, T. Ng, S. Vasudevan “Plasma Actuators for Hingeless Aerodynamic Control of an Unmanned Air Vehicle” AIAA Paper 2006-3495, 3rd AIAA Flow Control Conference, San Francisco, California, June 5-8, 2006.
- <sup>5</sup>T. Corke, M. Post “Overview of Plasma Flow Control: Concepts, Optimization, and Applications” AIAA Paper 2005-563, 43rd AIAA Aerospace Sciences Meeting & Exhibit, Reno, Nevada, January 10-13, 2005.
- <sup>6</sup>M. Munská, T. McLaughlin “Circular Cylinder Flow Control Using Plasma Actuators” AIAA Paper 2005-141, 43rd AIAA Aerospace Sciences Meeting & Exhibit, Reno, Nevada, January 10-13, 2005.
- <sup>7</sup>T. Jukes, K. Choi “Turbulent Boundary-Layer Control for Drag Reduction Using Surface Plasma” AIAA Paper 2004-2216, 2nd AIAA Flow Control Conference, Portland, Oregon, June 28-1, 2004.
- <sup>8</sup>A. Vorobiev, R. Rennine, E. Jumper “An Experimental Investigation of Lift Enhancement and Roll Control Using Plasma Actuators” AIAA Paper 2006-3383, 37th AIAA Plasmadynamics & Lasers Conference, San Francisco, California, June 5-8, 2006.
- <sup>9</sup>G.I. Font, S. Jung, C.L. Enloe, T.E. McLaughlin, W.L. Morgan, J.W. Baughn “Simulation of the Effects of Force and Heat Produced by a Plasma Actuator on Neutral Flow Evolution.” AIAA Paper 2006-167, 44th AIAA Aerospace Sciences Meeting & Exhibit, Reno, NV, January 2006.
- <sup>10</sup>Y.B. Suzen, P.G. Huang “Simulations of Flow Separation Control using Plasma Actuators.” AIAA Paper 2006-877, 44th AIAA Aerospace Sciences Meeting & Exhibit, Reno, NV, Jan. 2006.
- <sup>11</sup>Y.B. Suzen, P.G. Huang, J.D. Jacob, D.E. Ashpis “Numerical Simulations of Plasma Based Flow Control Applications.” AIAA 2005-4633, 35th AIAA Fluid Dynamics Conference & Exhibit, Toronto, Ontario Canada, June 2005.
- <sup>12</sup>Suzen, Y.B., Huang, P.G., “Numerical Simulation of Unsteady Wake/Blade Interactions in Low Pressure Turbine Flows Using an Intermittency Transport Equation,” Journal of Turbomachinery, Vol. 127, No. 3, pp. 431-444, July 2005.
- <sup>13</sup>Suzen, Y.B., Huang, P.G., “Comprehensive Validation of an Intermittency Transport Model for Transitional Low-Pressure Turbine Flows,” The Aeronautical Journal, Vol. 109, No. 1093, pp. 101-118, March 2005.
- <sup>14</sup>Jacob, J.D., Ramakumar, K., Anthony, R., Rivir, R.B., “Control of Laminar and Turbulent Shear Flows Using Plasma Actuators,” Fourth International Symposium on Turbulence and Shear Flow Phenomena, TSFP-4, Williamsburg, VA, June 2005.
- <sup>15</sup>Chen, H., Huang, P.G., and LeBeau, R.P., “A Cell-Centered Pressure Based Method for Two/Three-Dimensional Unstructured Incompressible Navier-Stokes Solver”, AIAA-2005-0880, 2005.